

Operability of Implantable Integrated Implants' Wireless Charging Device and Biotelemetric System

Alexey Rabin, Anastasia Petrushevskaya

Saint Petersburg State University of Aerospace Instrumentation
Saint Petersburg, Russian Federation
alexey.rabin@guap.ru, aap@guap.ru

Abstract—This article discusses the well-known inductive wireless power transfer for implantable devices. These devices are intended for use in the area of medicine, pharmacology and human physiology. Currently existing bioimplants need to be periodically removed from a body to replace a source of energy supply and then reinstall them in a body. It is to a certain degree a threat to the health of the patient and degrades the quality of his life. Developed by the authors wireless charger for transcutaneous energy supply of implantable modules automatically adjusts the power of the electromagnetic field. It gives the possibility to use either non-rechargeable power sources or batteries charged via wireless power transmission. The methodology for assessing the impact of the energy fields of experimental prototype of implant power supplies' wireless charging on biological objects is presented. This solution minimizes the heating of the receiving module, both in the area of the receiving circuit, and in the area of the stabilizer of the charging current of the battery. The integration scheme of experimental prototypes of wireless charging device and implantable biotelemetric system is considered. The theoretical analysis of the impact of the energy fields on biological objects is fulfilled. Three consistent tests of integrated charging device and implantable biotelemetric system are discussed. Testing of operability of the wireless charging device at integration with the implantable biotelemetric system is considered in details. The tests' results verified the compliance of the specified parameters with the theoretical relations and the requirements of the technical specification.

I. INTRODUCTION

One of the tasks of the future medicine are a creation and an implementation of the personalized medicine in practice, the basis of which will be an individual approach for each patient, including prevention, diagnosis and continuous monitoring of the health status.

The interest in the researchers' environment in the development and use of biotelemetric systems (BTS) for remote health monitoring is related to the fact that, due to their miniaturization while expanding functional qualities, practical medicine receives new technologies.

However, in practice, the implementation of remote monitoring of livelihoods faces several problems. Implantable devices are introduced into a human body surgically, and they autonomously monitor the functioning of individual organs and systems. The currently existing bioimplants need to be periodically removed from a body to replace a source of energy supply and then reinstall them in a body. To a certain extent, this poses a threat to the patient's health and impairs his quality

of life. It is to a certain degree a threat to the health of the patient and degrades the quality of his life [1], [2].

Thereby, the priority task is the development of a wireless charging device for a percutaneous energy supply of implantable modules, as well as the development of a methodology for assessing the impact of the energy fields of experimental prototypes on biological objects. When solving this urgent task, it is necessary to ensure high efficiency wireless energy transfer, regardless of the implant location in the patient's body [3].

An additional analysis of scientific and technological achievements in the development of remote monitoring systems for the patient's functional state, created on the basis of wireless implantable biotelemetry, confirmed the relevance of the chosen research area and its compliance to the current level of development of this type of equipment, as well as outlined the problems that need to be solved to achieve the stated goals.

II. EXPERIMENTAL PROTOTYPE OF THE IMPLANTABLE WIRELESS CHARGING DEVICE

The developed wireless charging device is intended to provide power for devices implantable in a biological object: depending on the functional purpose, to provide wireless recharge of implant batteries or wireless power supply of non-accumulator implants.

At the beginning of design of the transmitting and receiving modules of the wireless power transmission device, it was necessary to study inductors of various types: cylindrical, toroidal, spiral, since the type of the electromagnetic field strength's distribution, as well as the type of the distribution of the coupling coefficient (or mutual inductance) of coils with their different relative positions. In addition, the manufacturing technology of transmitting and receiving inductors, which allows the possibility of their production both through manual or automated winding from wire, and using a conductive pattern of a printed circuit board, was analyzed.

The experimental prototype of the wireless charging device of implants' power supply sources consist of the receiving and transmitting modules and is shown in Fig. 1 and Fig. 2, respectively [4].

The transmitting module sets the operating frequency and provides a change in the power of the force field to correct the output power level of the receiving module. Fig. 3 shows the general view of both modules of the charging device.

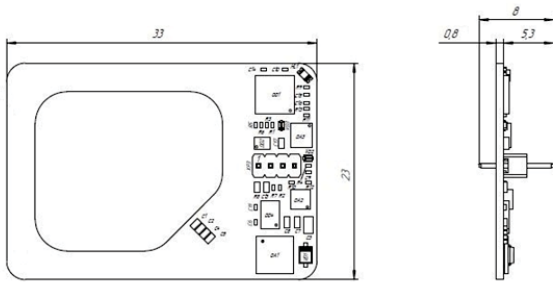


Fig. 1. General drawing of the wireless charging device. Receiving module

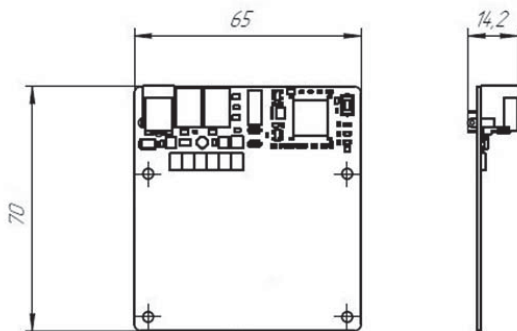


Fig. 2. General drawing of the wireless charging device. Transmitting module

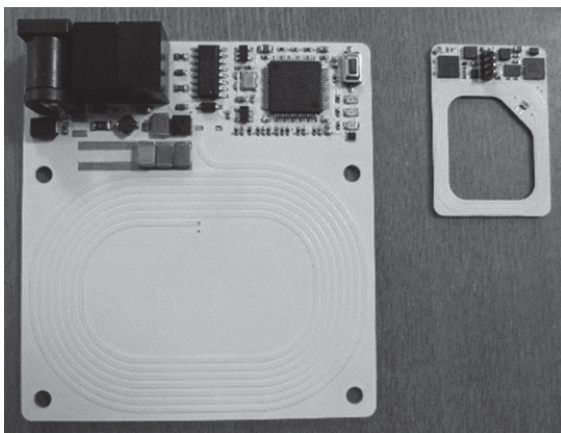


Fig. 3. Transmitting (left) and receiving (right) modules of the charging device

III. EXPERIMENTAL PROTOTYPE OF THE IMPLANTABLE BIOTELEMETRIC SYSTEM

The developed modules of the wireless charging device should be used in conjunction with an implantable BTS in order to assess the impact of wireless energy transfer method based on electromagnetic induction on a biological object.

The BTS is intended for testing in biological objects and should transmit electrocardiogram (ECG), electromyography (EMG), temperature, accelerometry signals, as well as parameters received from the receiving module of the charging device: housing temperatures and the receiving module, the voltage on the battery during charging, charging current.

The experimental prototype of the implantable BTS also consist of the receiving and transmitting modules and is shown in Fig. 4 and Fig. 5, respectively [4].

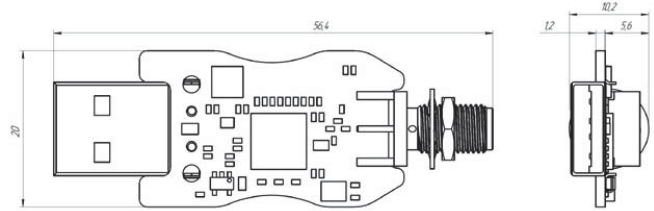


Fig. 4. General drawing of the implantable BTS. Receiving module

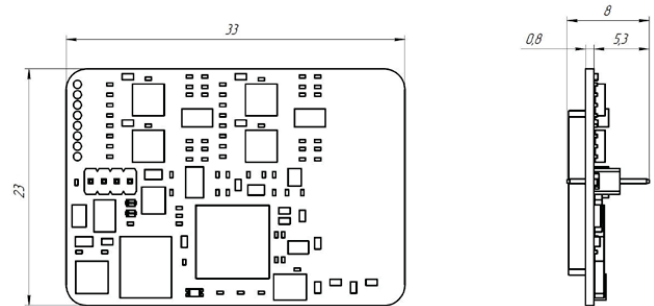


Fig. 5. General drawing of the implantable BTS. Transmitting module

Fig. 6 shows the general view of both modules of the BTS.

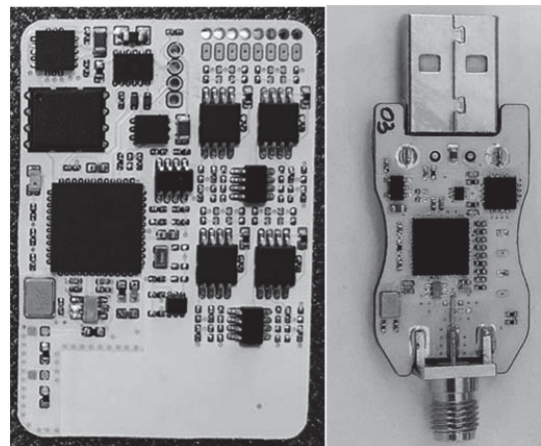


Fig. 6. Transmitting (left) and receiving (right) modules of the BTS

IV. INTEGRATION OF THE WIRELESS CHARGING DEVICE AND THE IMPLANTABLE BIOTELEMETRIC SYSTEM

The receiving module of the charging device through the board-to-board connector is connected to the transmitting module of the BTS, which, when encapsulated, can be placed inside a biological object. Charging device's transmitting module is placed on the body of a biological object opposite the charging device's receiving module and generates an electromagnetic field, the energy of which is converted at the last to charge a rechargeable power source (battery, supercapacitor) of the BTS' transmitting module.

Receiving module of charging device and transmitting module of BTS have a shape with rounded corners, consistent with each other and allowing them to work together. Due to the board-to-board connector, the receiving module of the charging device is located in the immediate vicinity of the printed circuit board of the transmitting module of BTS, through which it is

connected to the battery or to an array of capacitors. Hermetically encapsulated products can then be implanted into a biological object at a depth that meets the stated technical specifications. Thus, in the process of modules integration, the complete modules are connected to each other into a single functional unit – an integrated charging device and BTS (Fig. 7).

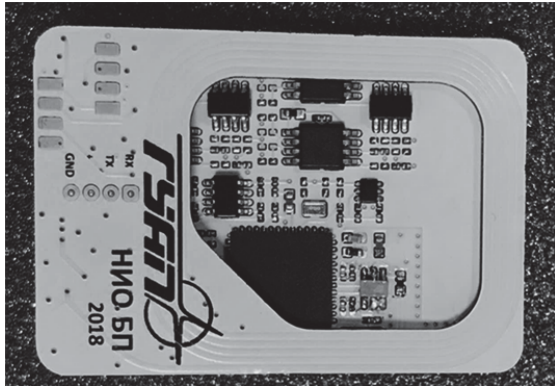


Fig. 7. Integrated charging device and BTS

For the implementation of the energy transfer the transmitting module antenna of the charging device should be placed outside the biological object on the same axis with the receiving module antenna of charging device. When power is connected to the transmitting module of the charging device, it begins to generate an alternating electromagnetic field, which allows to obtain at the output of the charging devices' receiving module sufficient power to charge the battery of the BTS' transmitting module.

The BTS receives and displays information on a PC for its further monitoring and analysis. Conceptual model is shown in Fig. 8.

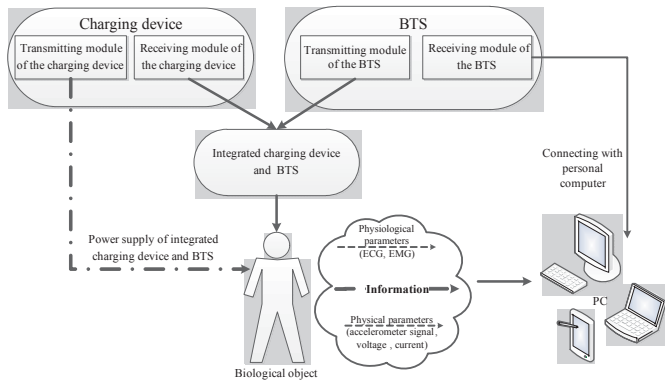


Fig. 8. Conceptual model of integration of wireless charging device and BTS

V. ANALYTICAL DESCRIPTION OF ASSESSING OF THE IMPACT OF THE ENERGY FIELDS ON BIOLOGICAL OBJECTS

For correct operation of contactless charging of experimental prototypes of implant power supply sources and prevention of excessive influence of energy fields on biological objects, magnetic constant and inductance

indicators were estimated by analytically calculating the value of the output current when the battery was charged.

To do this, it was necessary to calculate the inductance of both circuits first [5]. The inductance of one turn, taking into account the winding radius r and the conductor diameter d when the condition $d/(2r) \ll 1$ is fulfilled, is calculated by the formula:

$$L(r, d) = \mu_0 r \left(\ln \left(\frac{4r}{d} \right) - 2 \right), \tag{1}$$

where $\mu_0 = 4\pi \cdot 10^{-7}$ H/m is the magnetic constant.

The mutual inductance of two round turns lying in parallel planes is described by the formula:

$$M(r_1, r_2, \rho, \delta) = \pi \mu_0 \sqrt{r_1 r_2} \int_0^\infty J_1 \left(x \sqrt{\frac{r_1}{r_2}} \right) \cdot J_1 \left(x \sqrt{\frac{r_2}{r_1}} \right) \times \\ \times J_0 \left(x \frac{\rho}{\sqrt{r_1 r_2}} \right) \cdot e^{-x \frac{\delta}{\sqrt{r_1 r_2}}} dx, \tag{2}$$

where ρ is the axial displacement between turns, s is the distance between the planes of the turns, J_0 and J_1 are the Bessel functions of the first kind.

The total inductance of two co-wound coils is defined as

$$L = L_1 + L_2 + M_{12} + M_{21}. \tag{3}$$

Then, according to the notation adopted in Fig. 9, and using formulas (1)-(3), the inductance L_c of a volume multi-turn cylindrical coil can be expressed:

$$L_c = N_l \sum_{i=1}^{N_w} L_i(r_i, d) + \sum_{n=1}^{N_l} \sum_{m=1}^{N_l} \sum_{i=1}^{N_w} \sum_{j=1}^{N_w} M \times \\ \times (r_{n,i}, r_{m,j}, 0, s | n - m |) \cdot a_{n,m,i,j}, \tag{4}$$

where N_l is the number of layers in a plane, N_w is the number of turns in the layer, $a = 0$, if $n = m$ and $i = j$, and $a = 1$, otherwise.

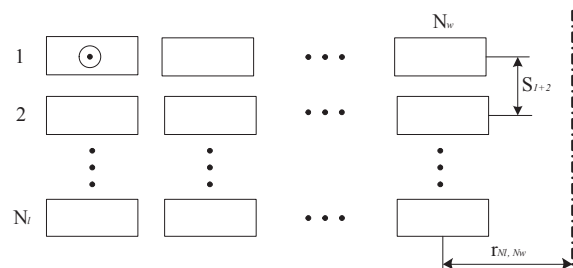


Fig. 9. Geometric parameters of inductors made on the printed circuit board

The inductance of a rectangular coil with rounded corners was determined by the formula (4) by introducing the parameter of equivalent radius r_{eq} of a cylindrical coil. The approximating function for calculating r_{eq} was chosen empirically. The boundary values of r_{eq} were determined by calculating the inductance over an equivalent area and perimeter of a rectangular coil, namely, r_{eqL} and r_{eqS} (equivalent radii), respectively, along the length and the area

of the middle turn, which were calculated using the formulas:

$$r_{eqL} = (r - w/2) + (a + b - 4r)/\pi, \quad (5)$$

$$r_{eqS} = \sqrt{((a - w)(b - w) + (\pi - 4)(r - w/2)^2)/\pi}. \quad (6)$$

As a result of the work, it was concluded that it is advisable to use spiral inductors made on a printed circuit board for both the transmitting and receiving modules, since this approach made it possible to fulfill the set requirements and achieve a high degree of reproducibility of the characteristics of the manufactured inductors.

At the same time, the research was made of the influence of coils' turns' configuration on the active component of the inductors' impedance, which revealed a significant effect of the turns' proximity. Along with the surface effect, it negatively affected the active resistance of the inductors as the resonant frequency of the device increased [6].

In addition, it was necessary to determine the resonance circuit, which could be implemented for both current resonance and voltage resonance. The design of various circuits demonstrated the feasibility of using a series resonance circuit in both modules of the device.

Equivalent radius was calculated by the formula:

$$r_{eq} = r_{eqL} - \left(1 - \frac{w}{r_{eqL} + w}\right)(r_{eqL} - r_{eqS}). \quad (7)$$

The calculated inductance values were 50.2 μH and 36.3 μH for the transmitting and receiving inductors, respectively.

The values of the coupling coefficient of the inductors k were calculated by the formula

$$k = \frac{M}{\sqrt{L_t L_r}}, \quad (8)$$

where M is the mutual inductance of coils, L_t и L_r are the inductances of transmitting and receiving inductors, respectively [7].

The mutual inductance between two flat coils can be calculated by replacing each of them with two turns, the radii of which are defined as $r_{\text{avg}} \pm w/8\sqrt{3}$, where r_{avg} was replaced by r_{eq} for rectangular inductors with rounded corners.

If the transmitting inductor is described by turns A and B , and the receiving one is described by C and D , then their mutual inductance can be described as

$$M \approx N_t N_r \frac{M_{AC} + M_{AD} + M_{BC} + M_{BD}}{4}, \quad (9)$$

where N_t и N_r are number of turns in one layer of inductors.

After calculating M using expressions (2) and (9), as well as the inductances of one layer of the coils (4) and placement of these values into (8), the distribution of k values was determined.

The calculation of the amplitude values of the current was made by the complex amplitudes' method. In general, the solution was reduced to a system of equations describing the equivalent circuit of the experimental facility:

$$\begin{cases} E_0 = i_1 \left(R_E + R_{L_t} + j\omega L_t + \frac{1}{j\omega C_t} \right) - i_2 \cdot j\omega M \\ i_1 \cdot j\omega M = i_2 \left(R_{L_r} + j\omega L_r + \frac{1}{j\omega C_r} + 2R_d + \frac{R_z R_{chg}}{R_z + R_{chg}} \right), \end{cases} \quad (10)$$

where ω is the operating frequency of the generator, E_0 and R_E are equivalent voltage and internal resistance of the generator's amplifier, i_1 and i_2 are currents in the transmitting and receiving circuits, R_{L_t} and R_{L_r} are the inductors' active resistance, C_t and C_r are the equivalent capacitance of resonant circuits calculated by the formula $C = 1/(\omega^2 L)$, based on the resonant frequencies of the circuits of the experimental facility, R_d is the resistance of the diode of the rectifier bridge, R_z is the resistance of the Zener diode, R_{chg} is the resistance of the charge control module [8].

E_0 was calculated based on the idling parameters of the transmitting part:

$$E_0 = I_0 \sqrt{(R_E + R_{L_t})^2 + \left(\omega L_t - \frac{1}{\omega C_t}\right)^2}, \quad (11)$$

where I_0 is the no-load current in the transmitting inductor.

In the process of developing a methodology for assessing the impact of the energy fields of experimental prototypes of contactless charging of implant power sources on biological objects along with the calculation of the resistance of diodes, the effect of temperature conditions of inductors on the stability of tuning circuits to resonance was investigated.

The resistance of the bridge diodes was expressed as

$$R_d(V) = V / \left(I_s \left(e^{\frac{qV}{nkT}} - 1 \right) \right), \quad (12)$$

where V is the diode voltage, $I_s = 830 \cdot 10^{-9}$ is the reverse saturation current, $n=1$ is the emission coefficient, k is the Boltzmann constant, T is the temperature (K), q is the elementary electric charge.

VI. RESULTS OF EXPERIMENTAL ASSESSING OF THE IMPACT OF THE ENERGY FIELDS ON BIOLOGICAL OBJECTS

The influence of the temperature conditions of the inductors on the stability of tuning the circuits in resonance was also investigated. To increase the stability of their work, capacitors of various form factors and from various dielectrics were tested. Among other things, the possibility of use of air trimmers, of lead-out ceramic capacitors' array for various installation technologies and different types of dielectrics was investigated. The question was relevant especially for the resonant circuit of the transmitting module due to its high quality and high amplitudes of its currents.

As a result, it was decided to abandon the use of air trimmers due to their high dimensions, cost and low operational reliability in favor of SMT ceramic capacitors with a NPO

dielectric. Finally, various schemes for constructing the amplifier of the transmitter module of the device were tested using analytical, model, and full-scale methods [7], [9]. As a result, the D class amplifier circuit was chosen (Fig. 10).

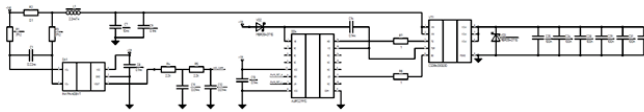


Fig. 10. D class amplifier circuit

VII. PREPARATION FOR INTEGRATED CHARGING DEVICE AND IMPLANTABLE BIOTELEMETRIC SYSTEM TESTING

The goal of the tests' sequence is the verification of the compliance of the specified parameters with the theoretical relations and the requirements of the technical specification.

During the full-scale tests of the charging device's modules, the influence of the load of the transmitting module's amplifier on obtaining the maximum output current at different relative positions of the transmitting and receiving inductors was also investigated, which made it possible to optimize the parameters of the key components of the circuit during their development. We also studied the influence of various elements of the receiving module of the charging device and the transmitting BTS' module on the efficiency of wireless energy transfer. As a result, an acceptable configuration for the order of connection of the components during their integration was chosen. At the same stage, various insulating materials with high magnetic permeability were tested to improve the operation parameters of the charging device.

The key elements of the charging device are transmitting and receiving inductors. The attainability of the required indicators was evaluated by analytical calculation of the value of the output current when the battery is charged. The required parameters of the inductors are presented in Table I.

TABLE I. PARAMETERS OF THE INDUCTORS

Parameter	Transmitting module's inductor	Receiving module's inductor
a – overall width, [mm]	62	25.5
b – overall depth, [mm]	45.5	22.4
r – overall radius of a rounding, [mm]	20.5	6.175
h – overall height of winding, [mm]	1	0.8
w – overall width of winding, [mm]	10	2.55
N – the number of turns (the number of layers and turns in them)	4×7	6×5
H – conductor's height, [microns]	35	35
W – conductor's width [μm]	1000	350

Two main approaches to solve the problem of implantable biotelemetric systems' power supply are considered in [3, 6, 10]. These are the usage of either non-rechargeable power

sources or batteries charged via wireless power transmission. Non-rechargeable power supplies are effective in the case of low power consumption along with the ability to ensure an adequate lifetime of the implantable system (pacemakers, subcutaneous cardiac monitors for short-term use). In the case of more resource-intensive multichannel stimulation tasks, telemetric collection of a set of parameters to achieve a sufficient period of operation, it is advisable to use a wireless power transmission.

Successful joint operation of the developed by the authors experimental prototypes of the wireless charging device of the implant batteries (wireless power supply of non-accumulator implants) and the BTS is confirmed by receiving a signal from the accelerometer sensor of the transmitting part of the BTS while testing, as well as the voltage and charge current of the battery on the device's receiving module are displayed on the screen of the personal computer monitor.

Physiological saline solution is currently regarded as one of the most common simulators of the internal environment of a biological object [2] in the laboratory testing. Physiological saline is understood to be aqueous solutions of salts in such a concentration that the osmotic pressure of the solution to be equal to the intracellular osmotic pressure of the body. Thus, the balance of osmotic pressure between the solution and body tissues is maintained [11]. Physiological solution is also called isotonic. In an isotonic solution, water molecules are excreted and absorbed by the cell in equal measure, which provides its normal functioning.

Most frequently used is a solution of sodium chloride in a concentration of 0.9%. This solution contains nothing but salt (sodium chloride) and water. This salt concentration is considered optimal to maintain the solution isotonic properties. It is a colorless transparent liquid slightly salty in taste.

Thus, the saline solution in the laboratory is prepared on the basis of sodium chloride. To prepare one liter of saline solution it is required 9 grams of salt and a liter of distilled water. Salt dissolves in water quickly enough. The resulting saline solution is suitable only for testing the technical characteristics of implantable devices. For the intravenous injections the implementation of such solution is absolutely inappropriate.

VIII. TESTING OF OPERABILITY OF THE WIRELESS CHARGING DEVICE AT INTEGRATION WITH THE IMPLANTABLE BIOTELEMETRIC SYSTEM

The testing of joint functioning of the integrated charging device and implantable BTS and the testing of operability of the BTS at integration with the charging device are considered in details in [12].

When activated transmitting module of BTS is placed in the simulation environment, on the computer screen, which is connected to the BTS' receiving module, signals are being visualized (battery voltage, accelerometry signal), indicating the overall correct functioning of the BTS in the simulation environment.

During the testing of joint functioning, the determined parameters of the integrated charging device and implantable BTS do not exceed the threshold values. Therefore, the objects

are considered to have passed this test.

During the testing of operability of the BTS at integration with the charging device insufficient common-mode rejection was noted, which caused further resistors correction.

Let's consider the test for verification the performance of the charging device at the integration with the BTS.

TABLE II. CHARGING DEVICE'S PARAMETERS AND ACCURACY OF THEIR MEASUREMENTS

Stage	Type of test (verification)	Units of measure	Nominal value	Max. deviation
1	Testing the direction and speed of data transfer between the transmitting and receiving modules of the charging device	baud	at least 1200	± 0,5%
2	Testing the power transmitted from the transmitting module to the receiving one	watt	at least 0.2	± 5%
3	Testing the battery charge current and power supply of non-accumulator implants	mA	at least 40	± 5%
4	Testing the characteristics of the charging device			
4.1	Testing the implant battery charge at a depth of at least 20 mm	mA	40	±5%
4.2	Testing the operation of the non-accumulator implant after turning off the force-field generator	sec.	10	0.5
4.3	Testing the possibility of changing the frequency and power of the force field	kHz	880	-

The frequency can be modified by replacing the clock frequency division factor of the microcontroller, but its final result should be equal to 880 kHz.

The power can vary from 0 to the maximum value, which is determined by the action of information coming from the receiving module of the charging device at a speed of at least 1200 baud. The power should be sufficient to provide a charging current of at least 40 mA at a voltage of at least 4.1 V.

The charging device's operability test consists of 4 main stages:

Stage 1. Testing the direction and speed of data transfer between the charging device's transmitting and receiving modules. Required values of indicators: speed of two-way data transfer between modules should be at least 1200 baud.

1.1 Connect the oscilloscope probes to the input 26 (PB0) of the microcontroller of the charging device's transmitting module.

1.2 Measure the modulation frequency of the recorded signal during the next communication session between the charging device's receiving and transmitting modules. (The received signal's change period should be no more than 0.833 ms, which corresponds to a data transfer rate of at least 1200 baud.)

Fig. 11. Test's stage 1 procedure

Stage 2. Testing the power transmitted from the charging device's transmitting module to the receiving module. Required values should be at least 0.2 W.

2.1 Place the charging device's transmitter and receiver modules using a micromanipulator at the distance of 20 mm from each other.

2.2 Connect a charged up to 50% battery to the XP3 connector of the receiver module board.

2.3 Connect the + 24 V power supply to the XP1 connector of the transmitting module.

2.4 Measure the temperature of the receiving antenna with the temperature recorder in order to prevent excessive heating of the surrounding tissues of the biological object for the device.

2.5 Using a digital multimeter, measure the output voltage and current at the output of the rectifier of the receiving module of the device. Calculate the current power value using the formula $P=U \cdot I$.
Repeat every 30 minutes until the battery is fully charged, i.e. until it receives a voltage of 4.1 V.

2.6 Continue operation of the charging device for 30 minutes.

2.7 Disconnect the +24 V power supply for the duration of the measurements according to claim 5 in order to prevent pickups arising as a result of the influence of the power EMF on the sensitive components of the meter. Then resume power.

2.8 Continue operation of the charging device for 30 minutes.

Fig. 12. Test's stage 2 procedure

Stage 3. Testing the amperage of the charge of the battery and the power of the battery-free implants. Required indicator value: battery charge current of at least 40 mA.

3.1 Connect the + 24 V power supply to the XP1 connector of the of the charging device's transmitting module.

3.2 Using the Agilent 34461A digital multimeter, measure the output voltage and current at the output of the rectifier DA1 of the receiving module of the Charging device. Calculate the current power value using the formula $P=U \cdot I$.

3.3 Instead of the battery, turn on the supercapacitor and measure the voltage across the capacitor. It must not exceed the voltage on a charged battery and is equal to 4.2 - 4.4 V.

Continue the modules for 30 minutes. Then repeat the measurement of the required indicators.

Fig. 13. Test's stage 3 procedure

Stage 4. Verification of the characteristics of the charging device.

The verified characteristics of the charging device are shown in Table III.

TABLE III. CHARACTERISTICS OF THE CHARGING DEVICE BEFORE THE IMPROVEMENT OF THE FILTERING OF THE SUPPLY VOLTAGE ON THE RECEIVING MODULE

The duration of the test, min	Temperature, °C	Battery charge, V	Battery charge current, mA	Power, watt	Speed of data transfer, baud	Voltage on the supercapacitor, V
0	23.17	3.86	46.98	0.180	2000	3.6
30	23.58	3.91	48.40	0.187	2000	3.8
60	24.26	3.84	48.37	0.191	2000	4.1
90	24.57	4.07	48.21	0.196	1000	4.2
120	24.51	4.10	49.35	0.204	1000	4.2
150	24.48	4.09	0.50	0.001	2000	4.2

During the test, spontaneous changes (decreases) in the data transmission rate by 2 times were revealed, the reason for which is an insufficient filtration of the supply voltage (increased ripple) of the microcontroller of the receiving module of the experimental prototype of the charging device.

The filtering of the supply voltage on the receiving module of the charging device has been improved. The evaluated characteristics of the charging device after this change are shown in Table IV.

TABLE IV. CHARACTERISTICS OF THE CHARGING DEVICE AFTER THE IMPROVEMENT OF THE FILTERING OF THE SUPPLY VOLTAGE ON THE RECEIVING MODULE

The duration of the test, min	Temperature, °C	Battery charge, V	Battery charge current, mA	Power, watt	Speed of data transfer, baud	Voltage on the supercapacitor, V
0	24.34	3.72	46.60	0.181	2000	3.7
30	25.39	3.88	47.33	0.189	2000	3.8
60	25.51	3.97	48.30	0.194	2000	4.1
90	25.59	4.10	49.94	0.200	2000	4.1
120	25.66	4.12	49.67	0.204	2000	4.2
150	25.62	4.11	0.83	0.003	2000	4.2

During the test, the voltage on the rechargeable battery increased from the initial value to the final charge voltage of 4.1-4.2 V, which confirms the regular joint operation of the integrated experimental prototypes of the charging device and the implanted BTS in the simulation environment of the biological object.

The combination of experimental prototypes of the charging device and the implanted BTS passed the technical tests.

IX. CONCLUSION

When implementing the methodology for assessing the impact of the energy fields of experimental prototype of implant power supplies' wireless charging on biological objects, it was decided to link the transmitting and receiving modules to negative feedback loop, which allows stabilizing the power supplied to the transmitting circuit by the D class amplifier. This solution minimizes the heating of the receiving module, both in the area of the receiving circuit, and in the area of the stabilizer of the charging current of the battery. Thus, in addition to smaller dimensions, the new solution allows optimizing the energy characteristics of the device as a whole.

Preventing of short-term negative effects on biological tissues is reduced to controlling its temperature and preventing the maximum permissible level from being exceeded. Considering the variability of the distance between the transmitting and receiving modules of the charging device due to the mobility of the biological object, the device of wireless energy transfer provides automatic adjustment of the electromagnetic field power to ensure the safety of the biological object.

Performing this research, technical tests of integrated charging device and implantable BTS were carried out, which verified the compliance of the specified parameters with the requirements of the technical specification.

At the beginning of work on the transmitting and receiving modules of the wireless power transmission device, it was necessary to study inductors of various forms [6]: cylindrical, toroidal, spiral, since the shape of the inductors influenced, in particular, on the distribution form of the electromagnetic field strength, as well as on the form of the distribution of the coupling coefficient (or mutual inductance) of the coils at their different mutual arrangement.

The experimental prototypes of the implantable BTS were tested to assess the performance of the device in biological objects (in the simulation environment of a biological object), which established the compliance of the test object with technical requirements. As a result of the tests, it was recommended to select the nominal values of the resistors to improve the reduction of the common mode interference.

The development of technical testing procedure of the integrated charging device and BTS allowed to check the joint operation of the modules of the charging device and the BTS and proved their normal functioning when working together.

The results of the tests confirmed the normal functioning of the integrated charging device and BTS.

ACKNOWLEDGMENT

The article was prepared in the course of applied research "Development of an experimental sample device for wireless charging of implant batteries" (unique identifier of the project RFMEFI57817X0233) of the Federal target program "Research and development in priority areas of development of the scientific and technological complex of Russia for 2014-2020" of the Ministry of Science and Higher Education of the Russian Federation in the priority direction "Life Science".

REFERENCES

- [1] J.S Ho , A.J. Yeh, E. Neofytou , “Wireless power transfer to deep-tissue microimplants”, *Proc. Nat. Acad. Sci. USA*. Vol. 111. No. 22, 2014, pp. 7974–7979.
- [2] P. Wright, “Energy harvesting in the human body”, *Implantable self-powered sensors*, New York: Emka PRESS, 2008, p. 215.
- [3] O. V. Gorskii Potential power supply methods for implanted devices Biomedical Engineering Volume 52, Issue 3, New York: Springer) 2018, pp. 204-209.
- [4] A. V. Rabin, M. A. Merkova and V. A. Kilimnik “Development of experimental prototype’s module functional schemes for battery wireless recharging implants”, *Proceedings of the workshop “Advanced Technologies in Material Science, Mechanical and Automation Engineering”*, Krasnoyarsk, 2019.
- [5] A. V. Rabin, A. A. Petrushevskaya, “Methods for assessing the impact of the energy fields of experimental prototypes of contactless charging of implants power supply sources on biological objects”, *IOP Conf. Series: Earth and Environmental Science*, vol. 315, 2019.
- [6] O. V. Gorskii, “The role of impedance matching for depth adjustment of inductive charger for medical implants”, *Proceedings of the 23rd Conference of Open Innovations Association FRUCT*, 2018, pp. 135-142.
- [7] N. Singhal, N. Nidhi, R. Patel, S. Pamarti, “A zero-voltage switching contour-based power amplifier with minimal efficiency degradation under back-off”, *IEEE Transactions on Microwave Theory and Techniques* vol.59, 2011, pp. 1589-1598.
- [8] A. A. Petrushevskaya , A. V. Rabin and V. A. Kilimnik “Energy fields' impact on biological objects”, *Proceedings of the 24th Conference of Open Innovations Association FRUCT*, 2019, pp. 328-334.
- [9] M. Ozen, R. Jos, C. M. Andersson, M. Acar, C. Fager, “High efficiency RF pulse width modulation of class-E power amplifiers”, *IEEE Transactions on Microwave Theory and Techniques*, vol.59, no.11, 2011, pp. 2931-2942.
- [10] A. V. Rabin, M. A. Merkova and V. A. Kilimnik, “Implantable biotelemetry system with extended functional capabilities”, *Proceedings of the 23rd Conference of Open Innovations Association FRUCT*, 2018, pp. 471-476.
- [11] R. Tashiro, R. N. Kabei, K. Katayama, “Development of an electrostatic generator that harnesses the motion of a living body” *Int. J. Jpn. Soc. Mechan. Eng.*, vol 43, 2000, pp. 916–922.
- [12] A. V. Rabin, A. A. Petrushevskaya, “Test methods for integrated experimental prototypes of wireless charging of implants’ power supply sources and implantable biotelemetric system”, *IOP Conf. Series: Earth and Environmental Science*, vol. 315, 2019.